Collisions of Slow Polyatomic Ions with Surfaces: Dissociation and Chemical Reactions of CD_5^+, $CD_4^{+\bullet}$, CD_3^+, and Their Isotopic Variants on Room-Temperature and Heated Carbon Surfaces†

Jana Roithová, Ján Žabka, Zdenek Dolejšek, and Zdenek Herman*

V. Čermák Laboratory, J. Heyrovský Institute of Physical Chemistry, Academy of Sciences of the Czech Republic, Dolejškova 3, 182 23 Prague 8, Czech Republic

Received: March 22, 2002; In Final Form: June 10, 2002

Interaction of small hydrocarbon ions, CD_3^+, CD_4^+, CD_5^+, and their isotopic variants CH_n^+ and $^{13}CH_n^+$ (n = 3, 4, 5), with room-temperature and heated carbon (highly oriented pyrolytic graphite, HOPG) surfaces was investigated over the collision energy range 16−52 eV. Mass spectra, translational energy distributions, and angular distributions of product ions were determined. Collisions with room-temperature surfaces showed both surface-induced dissociation of the projectiles and chemical reactions with the surface material. All projectiles showed formation of $C_2X_3^+$ (X = H, D) in interaction of the projectiles with terminal CH_3− groups of surface-adsorbed hydrocarbons and a small amount of C_3 product ions, and collisions of CD_4^+ led, in addition, to CD_4H^+ by H-atom transfer from surface hydrocarbons. The surface collisions were inelastic with 41−55% of incident energy in product-ion translation (incident angle 60° with respect to the surface normal). Heating of the surface to 600° C practically removed the surface hydrocarbon layer. Interactions of the projectiles with the heated surface showed then only dissociation of the projectile ions (no chemical reactions) in inelastic collisions with about 75% of the incident energy in product-ion translation. The ion survival probability was estimated to about 10% for CD_5^+ and about 30−60 times smaller (0.2−0.4%) for CD_3^+ and CD_4^+.

1. Introduction

Collisions of ions with surfaces offer an opportunity to study a broad range of chemical and physical processes. Over the past 15 years, considerable interest has been devoted to studying selected physical and chemical processes stimulated by impact of slow ions on surfaces.[1−3] As slow ions, one usually regards hyperthermal ions of energies about 1−100 eV. In this energy regime, the relative collision energy is of the same order of magnitude or somewhat larger than chemical-bond energies. The ion−surface interaction is thus large enough to lead to bond dissociation and yet not too large to obscure the chemical nature of it. Slow ion collisions with surfaces are finding many applications in science and technology and can provide useful information on the nature of both projectiles (especially polyatomic ones) and surfaces, as well as on the characteristics of ion−surface interactions.

Ion−surface collisions offer important information relevant to plasma-wall interactions in electrical discharges and fusion systems.[4] Hyperthermal plasma particles may collide with solid surfaces such as limiters and divertors in fusion devices, eroding the material by chemical and physical processes. Charged and neutral particles emitted from the surface may interact with the plasma and hit the surfaces again. In fusion devices, carbon is widely used as the material exposed to plasma and lack of data on ion−surface collisions, in particular, on collisions of slow molecular ions such as hydrogenic species and small hydrocarbon ions, has been repeatedly emphasized.

In our recent papers, we used the ion−surface scattering method to obtain information on energy partitioning in collisions of polyatomic ions with various surfaces, namely, surfaces covered by various self-assembled monolayers,[5] stainless steel covered by hydrocarbons,[6,7] and various carbon surfaces.[8] In this paper, we describe our results on scattering studies of collisions of small hydrocarbon ions (CD_5^+, $CD_4^{+\bullet}$, CD_3^+, and their H or ^{13}C isotopic variants) impinging on heated and nonheated highly oriented pyrolytic graphite (HOPG) surfaces. We describe the results of measurements of mass spectra and angular and translational energy distributions of the ion products. Analysis of the data makes it possible to estimate the ion survival probability and to describe the projectile dissociation processes and chemical reactions with the surface material.

Dissociation of small hydrocarbon, CH_n^+, and fluorocarbon, CF_n^+ (n = 1, 2, ...), ions on aluminum surfaces was studied earlier to gain insight into surface processes in plasma processing. [9] Significant charge neutralization (survival of about 0.3% for CH_n^+), dissociation of projectiles, and kinetic energies of fragments lower than 10 eV were observed for incident projectile energies up to 150 eV. Dissociative collisions of hydrogen ions and small hydrocarbon C_1−C_3 ions on a stainless steel (hydrocarbon-covered) surface have been recently under study in Innsbruck.[10] A number of studies have been performed on dissociative scattering of diatomic or small polyatomic (3−4 atoms) ions from single-crystal or liquid surfaces with energy and angular analysis of the product ions. Negative ion formation in collisions of hyperthermal, state-selected NO^+ with O/Al(111)[11] and OCS^+ with Ag(111)[12] was investigated, and conclusions about the mechanism were made. Dissociative scattering of 50−250 eV fluorocarbon ions, CF_n^+ (n = 1−3),

† Part of the special issue "John C. Tully Festschrift".

* To whom correspondence should be addressed. E-mail: zdenek.herman@jh-inst.cas.cz.

10.1021/jp025811z CCC: $22.00
Published on Web 06/26/2002

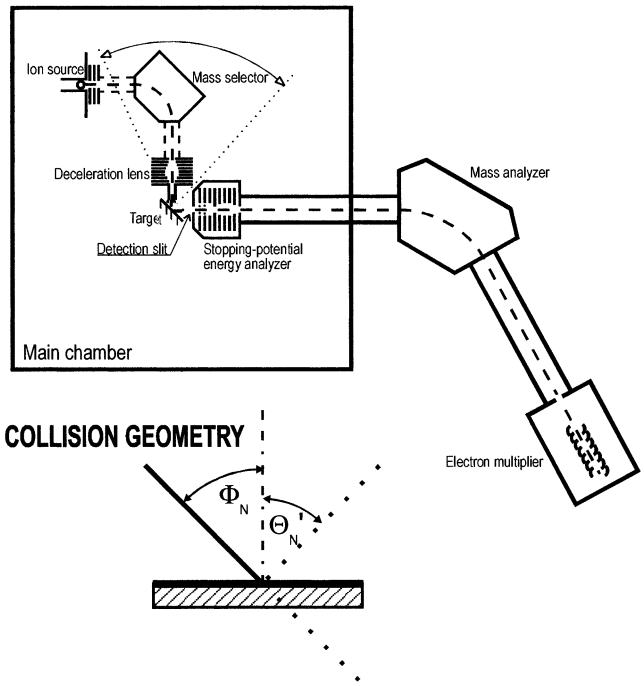

Figure 1. Schematics of the experimental setup. Inset defines the collision geometry.

from surfaces covered by perfluoropolyether liquid film[13−15] was interpreted on the basis of elastic scattering from the surface-layer terminal group.

Changes in slow ion scattering and energy transfer for clean versus adsorbate-covered graphite surfaces have been described for collisions of fullerene ions.[16] The extent of fragmentation, kinetic energy of the scattered ions, and chemical reactions (C_2 pick up on hydrocarbon-contaminated HOPG surface) changed dramatically after cleaning the surface by heating to 1000 °C. Examples of pick-up chemical reactions of incident ions with surface material have been described; the results have been summarized in excellent reviews.[2,3] Significant changes in product-ion kinetic-energy distributions and the extent of incident-to-internal energy transfer were observed in scattering studies of $Si(CH_3)_3^+$ collisions with clean Au(111) surface and Au surface covered by hydrocarbon C_6 self-assembled monolayer.[17]

2. Experimental Section

The experiments were carried out using the Prague beam-scattering apparatus EVA II modified for the ion−surface collision studies[6] (Figure 1). In the present experiments, projectile ions were formed by bombardment of methane molecules (CD_4, CH_4, $^{13}CH_4$) at a pressure of about 10^{-4} Torr in the ion source by 120 eV electrons (to ensure sufficient production of CD_5^+). The ions were extracted, accelerated to about 200−330 eV, mass analyzed by a 90° permanent magnet, and decelerated to a required energy in a multielement deceleration lens. The resulting beam had an energy spread of 0.2 eV, full width at half-maximum (fwhm), angular spread of 2°, fwhm, and geometrical dimensions of 0.4×1.0 mm^2. The beam was directed toward the carbon target surface under a preadjusted incident angle, Φ_N. Ions scattered from the surface passed through a detection slit (0.4×1 mm^2), located 25 mm away from the target, into a stopping potential-energy analyzer. After energy analysis, the ions were focused and accelerated to 1000 eV into a detection mass spectrometer (a magnetic sector instrument) and detected with a Galileo channel multiplier. The primary beam exit slit, the target, and the detection slit were kept at the same potential during the experiments, and this equipotential region was carefully shielded by μ-metal sheets. The primary beam−target section could be rotated about the scattering center with respect to the detection slit to obtain angular distributions.

The energy of the projectile ions was measured by applying to the target a potential exceeding the nominal ion energy by about 10 eV. The target area then served as a crude ion deflector directing the projectile ions into the detection slit. Their energy could be determined with accuracy better than about 0.2 eV. The incident angle of the projectile ions was adjusted before an experimental series by a laser beam reflection with a precision better than 1°. Incident (Φ_N) and scattering (Θ'_N) angles were measured with respect to the surface normal (see inset in Figure 1).

The carbon surface target was a 5×5 mm^2 sample of highly oriented pyrolytic graphite (HOPG) from which the surface layer was peeled off immediately before placing it into vacuum. The sample was mounted into a stainless steel holder located 10 mm in front of the exit slit of the projectile ion deceleration system. The thickness of the sample holder made angular measurements at scattering angles smaller than about 3° of the surface parallel difficult (scattering angles 87°−90°). The carbon target surfaces in the experiments were kept either at ambient temperature or at an elevated temperature of about 600 °C. For this purpose, the carbon surface could be resistively heated to about 1000 °C; its temperature was measured by a thermocouple and by a pyrometer. Practical absence of chemical reactions with surface hydrocarbons indicated that heating the surface to 600 °C decreased the concentration of hydrocarbons on the surface more than 100 times. This temperature was then regarded as sufficiently high to essentially remove the hydrocarbon (multi-) layer, which covered the HOPG surface at the room temperature (see ref 8 and also further on, sections 3.3 and 3.4).

The scattering chamber of the apparatus was pumped by a 2000 L/s diffusion pump (Convalex polyphenyl ether pump fluid), and the detector was pumped by a 65 L/s turbomolecular pump; both pumps were backed by rotary vacuum pumps. The background pressure in the apparatus was about 5×10^{-7} Torr; during the experiments, the pressure was about 5×10^{-6} Torr because of the leakage of the source gas into the scattering chamber.

3. Results and Discussion

3.1. Mass Spectra. Mass spectra of product ions resulting from the interaction of projectile ions with the nonheated or heated carbon (HOPG) surface are summarized in Table 1. Ion intensities are given as percent fractions of the total ion intensity recorded at m/z 12−45, $I_{rel} = 100I_i/(\sum I_i)$. However, because the survival probability of CD_5^+, its isotopic variants, and the respective dissociation products was found to be about 30−60 times higher than that of CD_3^+ or CD_4^+, while the abundance of the C_2 and C_3 groups of product ions was comparable for all projectiles, the spectra of CD_5^+ are normalized to 1000 rather than to 100 to have the C_2 and C_3 groups comparable for all projectiles (italics in Table 1). The projectile ions were CD_3^+, $CD_4^{+\bullet}$, and CD_5^+; complementary spectra were taken with projectiles CH_3^+, $CH_4^{+\bullet}$, and CH_5^+ and $^{13}CH_3^+$, $^{13}CH_4^{+\bullet}$, and $^{13}CH_5^+$. The spectra were measured for three incident energies of the projectiles, 16.6, 31.6, and 51.6 eV. The incident angle of the projectiles was $\Phi_N = 60°$ (i.e., 30° with respect to the surface), and the spectra were measured at the angular maximum

TABLE 1: Summary of Mass Spectra of Ion Product from Collision of Projectile Ions with Carbon HOPG Surfaces at Room Temperature and Heated to 600 °C (H)[a]

energy		products (*m*/*z*)																					
(eV)	projectile	13	14	15	16	17	18	20	21	22	26	27	28	29	30	31	38	39	40	41	42	43	45
16.6	CD_3^+		2.6		5.2	1.8	62.6					3.1	5.6	12.1	3.9		0.3		1.3	0.9		1.0	
	CD_3^+(H)		4.6		9.6		85.8																
	CH_3^+	1.1	3.5	66.8	2.3						1.0	16.0	2.6	2.6				2.1		0.5		1.8	
31.6	CD_3^+		5.5	1.1	14.8	8.6	49.8					5.6	6.9	5.8	1.6								
	CD_3^+(H)		8.7		32.2		59.1																
	CH_3^+	2.4	7.1	32.4	1.1						4.6	23.7	2.4	5.3	0.9		0.5	9.0		7.0		3.9	
	$^{13}CH_3^+$		1.8	12.9	27.0	0.2						14.8	15.6	11.5	2.1			2.0	4.3	5.3	1.8	0.8	
51.6	CD_3^+		4.4	4.0	11.4	11.0	21.1				4.4	11.1	7.7	8.6	2.9		0.6	5.4	1.9	2.3	0.8	2.7	
	CD_3^+(H)		11.7		43.2		45.0																
	CH_3^+		14.3	20.0		12.5					11.3	24.9						12.8		4.2			
16.6	CD_4^+				1.9	37.6	40.2	14.3	2.4			0.2	1.0	1.5	0.9								
	CD_4^+(H)				8.4		27.6	56.2	7.8														
	CH_4^+		5.7	72.3	8.9	4.0						5.9		1.5				0.4		1.0		0.4	
	$^{13}CH_4^+$			13.1	53.6	16.9	6.2					0.3	4.3	1.8	0.9				0.3	0.9	0.7	0.6	0.3
31.6	CD_4^+		0.7	0.7	5.1	32.7	36.6	10.6	0.3		0.2	2.4	2.7	3.9	0.9			0.8	0.6	1.2	0.3	0.2	
	CD_4^+(H)		3.9		20.9		47.8	27.5															
	CH_4^+	1.1	6.1	50.4	14.1						1.4	15.1	1.0	2.9				3.7	0.6	3.0	0.2	0.7	
	$^{13}CH_4^+$		1.3	15.2	45.5	6.5	1.2					5.8	10.2	5.4	1.6			1.0	2.1	2.5	0.9	1.1	
51.6	CD_4^+		0.9	2.7	8.6	32.9	33.1	2.3	2.2		0.9	5.3	3.2	3.5	0.4			0.8	0.9	1.6	0.2	0.5	
	CD_4^+(H)		8.2		37.0		50.4	4.5															
16.6	CH_5^+			*520*		*471*						*1.4*	*0.3*	*1.3*						*0.9*		*0.7*	
	$^{13}CH_5^+$				*479*		*517*					*1.0*	*0.3*	*1.4*	*0.2*	*0.2*				*0.3*	*0.2*	*0.3*	
31.6	CD_5^+						*758*			*223*		*4.4*	*2.8*	*7.1*	*3.4*					*1.2*		*0.5*	
	CH_5^+			*848*		*131*					*0.6*	*10.9*	*0.9*	*4.4*				*2.0*	*0.1*	*2.6*	*0.1*	*0.6*	
	$^{13}CH_5^+$				*789*		*185*					*5.2*	*7.4*	*5.5*	*1.5*			*1.2*	*1.5*	*1.7*	*0.5*	*1.0*	
51.6	CD_5^+					*25*	*813*			*59*	*2*	*34*	*20*	*20*				*9*	*9*	*10*			
	CD_5^+(H)						*909*			*91*													

[a] The intensities are normalized to total intensity of 100 (for CD_5^+ projectiles, normalized to 1000, respective numbers in italics; see also text).

of the product ions or close to it at $\Theta'_N = 74°$ (i.e., 16° with respect to the surface). The relative ion intensities in Table 1 are usually averages of a series of recording of mass spectra, and thus, they may differ slightly from intensities in the sample mass spectra as shown in Figures 2 and 6.

The spectra with the carbon surface at room temperature showed a considerable amount of product ions formed in chemical reactions with the surface material. Product ions $C_2X_n^+$ and $C_3X_n^+$ (X = H, D) were formed in collisions of all projectile ions. In addition, in collisions with the molecular radical cation $CD_4^{+\bullet}$ ($CH_4^{+\bullet}$), formation of the product of the H-atom transfer reaction with the surface hydrogen CD_4H^+ (CH_5^+) and its dissociation products was observed. This confirmed our earlier finding[8] that at room temperature a layer of hydrocarbons covered the carbon surface. When the surface was heated to 500 °C or higher, the amount of these reaction products decreased by a factor of at least 100. We conclude, therefore, that this heating removed the layer of hydrocarbons and the collision took place with a largely hydrocarbon-free surface of HOPG. The spectra of product ions resulting from collisions of the projectile ions with the HOPG surface heated to 600 °C are denoted in Table 1 by (H), and further scattering results will be discussed in section 3.3. Cooling of the heated surface to room temperature led to reestablishing the hydrocarbon layer on the surface after about 2−3 h and repeated heating again to its practical removal. The mass spectra and other scattering results after these heating−cooling circles were reproducible within the experimental error.

3.2. Ion Survival Probability. The main process in the interaction of a projectile ion and a surface is neutralization of the projectile, as shown by numerous studies.[1] The ion survival probability, S_a (percentage of ions surviving the surface collision), is defined as the ratio of the sum of intensities of all product ions scattered from the target, $\sum I_{PT}$, to the intensity of the projectile reactant ions incident on the target, I_{RT}, $S_a = 100\sum I_{PT}/I_{RT}$. While I_{RT} was measured in the experiments reported here, $\sum I_{PT}$ could not be directly determined and had to be estimated from the sum of intensities of product ion reaching the detector, $\sum I_{PD}$, taking into account the discrimination of the apparatus (D_A) and the angular discrimination of the scattering differential measurements ($D(\omega)$). A direct measurable quantity was the relative survival probability, $S_{eff} = \sum I_{PD}/I_{RT}$, related to S_a (expressed in percent survival) by $S_a = 100FS_{eff}$, where F summarizes the discrimination effects.

It holds for the intensity of the projectile (reactant) ion (R) registered on the detector (I_{RD}) and incident on the target (I_{RT})

$$I_{RD} = D_A D(\omega)_R I_{RT} \quad (1)$$

and analogously for the scattered product ions (P)

$$I_{PD} = D_A D(\omega)_P I_{PT} \quad (2)$$

For the estimation of the angular discrimination of the reactant beam, $D(\omega)_R$, and the scattered product-ion beam, $D(\omega)_P$, the following simplifications were made: (1) The area of the detection slit (0.4 × 1.0 mm^2) was approximated by an aperture of the same area (diameter 0.72 mm, angular acceptance $\Theta_{ds} = 1.6°$). (2) The angular distribution of the reactant beam was approximated by its full width at half-maximum (fwhm), Θ_R(fwhm) = 2.0°. (3) The angular distribution of the scattered product beam was approximated by an average of fwhm of several typical product-ion distributions (see later), Θ_P(fwhm) = 14°. The angular discrimination was then approximately estimated as $D(\omega)_R = \Theta_{ds}^2/\Theta_R^2$(fwhm) = 0.64 and $D(\omega)_P = \Theta_{ds}^2/\Theta_P^2$(fwhm) = 0.013.

By putting a potential on the target (see above, section 2), one can deflect the reactant ion beam into the detection slit, measure its angular distribution, and register it on the output of the detector multiplier (includes amplification by the multiplier). The respective intensities were $I_{RT} = 1.7 \times 10^{-9}$ A and $I_{RD} =$

TABLE 2: Percentage of Surviving Ions, S_a (%), in Collisions of CD_3^+, $CD_4^{+\bullet}$, and CD_5^+ with Heated (H) and Nonheated HOPG Carbon Surfaces for Three Incident Energies[a]

	$E_{inc} = 16.6$ eV		$E_{inc} = 31.6$ eV		$E_{inc} = 51.6$ eV	
projectile	S_a (%)	$S_{eff} \times 10^3$	S_a (%)	$S_{eff} \times 10^3$	S_a (%)	$S_{eff} \times 10^3$
CD_3^+	0.12 ± 0.03	2.15 ± 0.5	0.22 ± 0.04	4.3 ± 0.8	0.26 ± 0.16	5 ± 3
CD_3^+ (H)	0.09	1.9			0.1	2.0
$CD_4^{+\bullet}$	0.37 ± 0.06	7.2 ± 1.2	0.34 ± 0.2	6.6 ± 4.2	0.27 ± 0.26	5.1 ± 5
$CD_4^{+\bullet}$ (H)	5	9.5	2.3	4.4		
CD_5^+	12.5 ± 5	240 ± 100	12.0 ± 5	230 ± 10	18 ± 7	350 ± 130
CD_5^+ (H)					23	440

[a] Incident angle $\Phi_N = 60°$.

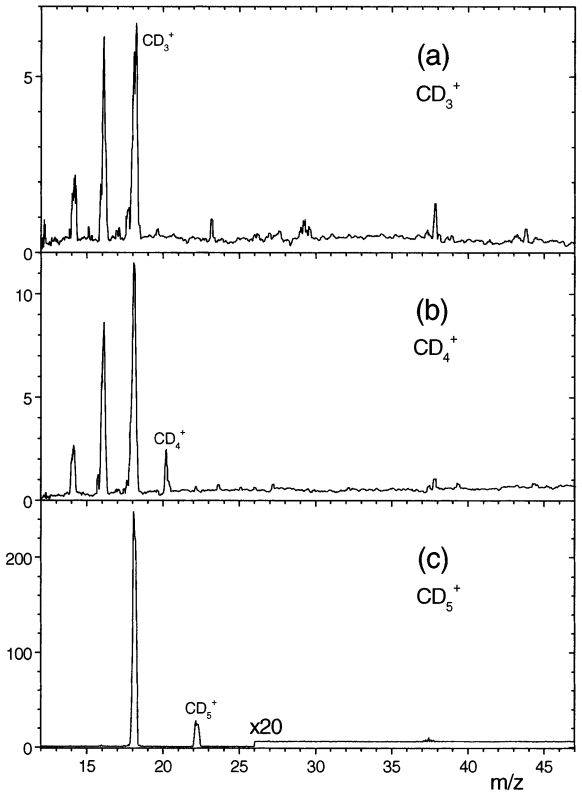

Figure 2. Mass spectra of product ions from collisions of (a) CD_3^+, (b) $CD_4^{+\bullet}$, and (c) CD_5^+ with a HOPG surface heated to 600 °C. Collision energy was 51.6 eV, and incident angle $\Phi_N = 60°$. Note increased sensitivity in part c for $m/z > 26$.

1.6×10^{-7}A. From the equations above, it follows that $F = I_{RT}D(\omega)_R/(I_{RD}D(\omega)_P) = 0.523$.

The values of S_{eff} obtained from the measured spectra and the values of S_a (estimated absolute survival in percent) are summarized in Table 2. The S_a estimates may be influenced by the inaccuracy of the simplified evaluation of the discrimination factors, but they provide a certain order-of-magnitude information. Though the values in Table 2 are mostly averages of measurements of many spectra, the standard deviation is rather large. The survival probability of the even-electron ion CD_5^+ is about 2 orders of magnitude higher than that of the radical cation $CD_4^{+\bullet}$ and that of the ion CD_3^+. The ion survival probability on clean heated carbon surface appears to be similar to that on the carbon surface covered by hydrocarbons.

3.3. Collisions with Heated HOPG Surface. Figure 2 shows samples of mass spectra of product ions obtained from collisions of the projectile ions CD_3^+, $CD_4^{+\bullet}$, and CD_5^+ impinging under $\Phi_N = 60°$ with incident energy of 51.6 eV on a HOPG surface heated to 600 °C. Only simple dissociation products of the projectiles, reflecting the loss of D atom or D_2 molecule (also a small amount of D + D_2 in case of $CD_4^{+\bullet}$) could be observed at this fairly high incident energy.

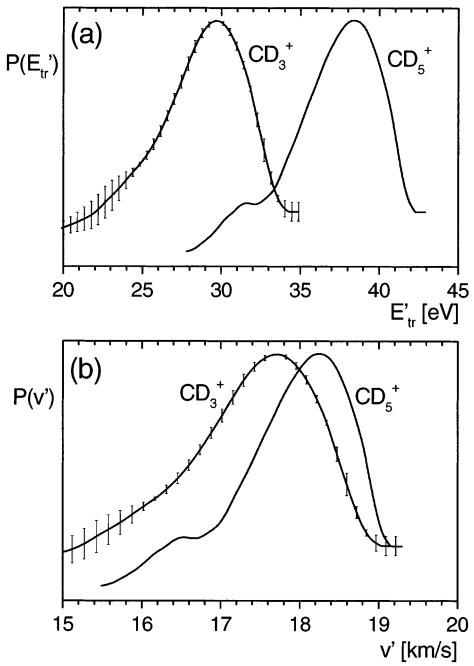

Figure 3. Distribution of (a) translational energy, $P(E'_{tr})$, and (b) velocity, $P(v')$, of product ions CD_5^+ (full line) and CD_3^+ (dashed line), both measured at $\Phi'_N = 74°$, from collisions of CD_5^+ with a HOPG surface heated to 600 °C. Incident energy was 51.6 eV, and incident angle $\Phi_N = 60°$.

Figure 3 summarizes the distribution of translational energies for the surface collisions of 51.6 eV CD_5^+ of the nondissociated product ion CD_5^+ and its only dissociation product CD_3^+ at their angular maxima. Both ions are inelastically scattered; the energy distribution of CD_5^+ peaks at 38.4 eV, at about 75% of the incident energy. The respective velocity distributions of the two product ions show peaking at almost the same velocity (CD_3^+ peaks at a velocity about 4% lower than that for CD_5^+) and suggest that the dissociation process of the surface-collision-energized projectile CD_5^+ is close to unimolecular decomposition after the interaction with the surface. Angular distributions of the two product ions are given in Figure 4: both ions exhibit a rather narrow distribution (about 13° fwhm) peaking at a subspecular angle $\Theta'_N = 72°$.

The extent of dissociation as obtained from the mass spectra of product ions upon impact of the projectile $CD_4^{+\bullet}$ can be used to estimate the distribution of energy converted in the surface collision into internal excitation of the projectile, $P(E'_{int})$. This approach was used earlier [5,6,8] and consists of using the break-down pattern of the projectile polyatomic ion to fit the relative intensities of the product ions by a trial-and-error distribution function. The break-down pattern of the projectile ion $CH_4^{+\bullet}$ ($CD_4^{+\bullet}$) is well-known both from experimental charge transfer[18,19] and threshold electron−photoion coincidence[20] studies and from quasi-equilibrium theory calculations.[21] Though $CH_4^{+\bullet}$

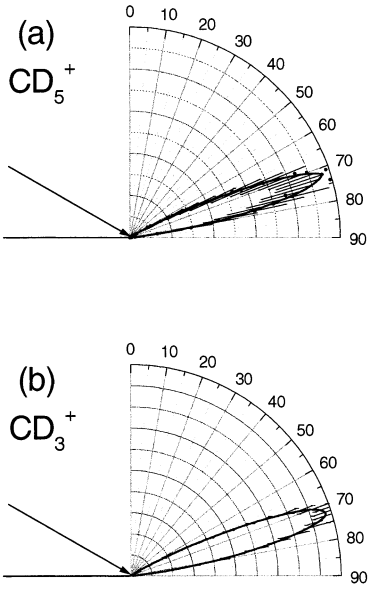

Figure 4. Angular distributions of product ions (a) CD_5^+ and (b) CD_3^+ from collisions of CD_5^+ with a HOPG surface heated to 600 °C. Incident energy was 51.6 eV, and incident angle $\Phi_N = 60°$.

is a rather small ion, it has been known to behave reasonably well as a polyatomic molecular ion with a high density of internal states. However, because of the simplicity of the break-down pattern (see Figure 5d), one can expect only an approximate information on $P(E'_{int})$. Also, the molecular ion CH_4^+ exhibits a rather large internal excitation energy from the ionization process, and this energy has to be taken into consideration as the initial internal excitation of the projectile ion. The distribution of the initial internal excitation energy was estimated from the photoelectron spectra of methane over the region of stability of the molecular ion CH_4^+ as given by the break-down pattern. The estimated distribution is plotted in Figure 5d as a dashed line; it ranges from zero to about 1.6 eV with a maximum at 0.8 eV.

The distribution of internal energy of the projectile ion $CD_4^{+\bullet}$, $P(E'_{int})$, that leads to its dissociation to fragments of the respective intensities after the surface collision is given for several collision energies in Figure 5. It peaks at increasingly higher incident energies of about 5−6% of the incident energy and exhibits a tailing to higher energies. The contributions to $P(E'_{int})$ come from the energy acquired from the surface during the collision and from the initial internal excitation of the projectile. However, it makes little sense to try to separate these two contributions, because $P(E'_{int})$ results from a multimode excitation in the surface collision during which energy between the projectile and the surface is exchanged. In fitting the experimental product-ion intensities to obtain $P(E'_{int})$ in Figure 5, the measured intensity of the fragment CD_2^+ was always higher than could be obtained by calculations with the use of the break-down pattern. This presumably reflects a certain deviation from the strictly unimolecular decomposition kinetics at high internal energies (above 5−6 eV) and a possible existence of isolated states in CH_4^+ high above the ionization potential.

The dashed line in Figure 5a shows $P(E'_{int})$ for collisions of $CD_4^{+\bullet}$ with nonheated (hydrocarbon-covered) HOPG surface (see section 3.4). Only at the incident energy of 16.6 eV, there was a significant difference in product-ion intensities with heated and unheated surfaces; for higher incident energies of 31.6 and 51.6 eV, these two product-ion intensities were very similar and could be fitted by one $P(E'_{int})$ curve, shown in Figure 5.

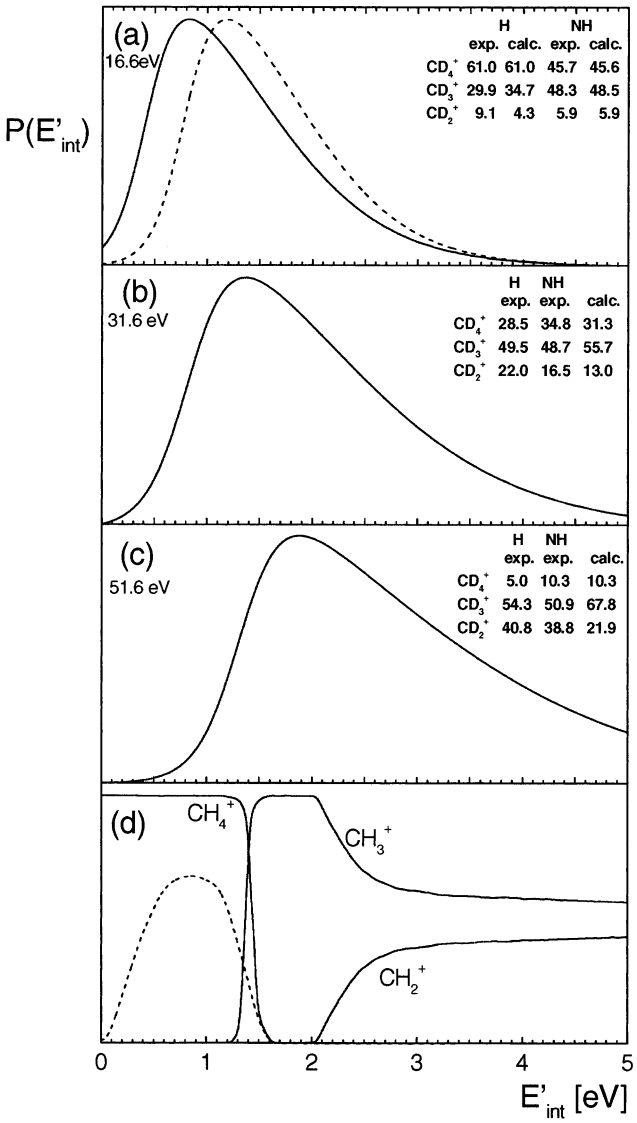

Figure 5. Distribution of energy transformed into the internal excitation of the projectile ion, $P(E'_{int})$, in surface collisions of $CD_4^{+\bullet}$ with heated (H) and room-temperature (NH, dashed) HOPG surfaces. Incident energies were (a) 16.6 eV, (b) 31.6 eV, and (c) 51.6 eV; incident angle $\Phi_N = 60°$. Panel d shows the break-down pattern of the molecular ion $CD_4^{+\bullet}$ used in the evaluation (dashed line shows estimated distribution of initial internal excitation of $CD_4^{+\bullet}$). Numbers show comparisons of measured ion abundance with calculated abundance resulting from the fits.

3.4. Collisions with HOPG Surface at Room Temperature (Nonheated Surface). Collisions of the projectile ions CD_3^+, $CD_4^{+\bullet}$, and CD_5^+ with the HOPG surface at room temperature show a dramatic change in the nature of product ions. Figure 6 shows examples of mass spectra obtained, if these projectile hit the surface with incident energies of 16.6 and 51.6 eV (i.e., lowest and highest incident energy investigated). Besides product ions that resulted from simple dissociation of the surface-energized projectile (CD_3^+, CD_2^+, CD^+), ions CD_4H^+ (low-energy collisions of $CD_4^{+\bullet}$), CD_2H^+, and ions $C_2X_n^+$ and $C_3X_n^+$ (X = H, D) appeared in the spectra with measurable intensities. These ions evidently resulted from interactions of the projectile with hydrogen and carbon of the surface material, and we concluded from it that at room temperature the HOPG surface was covered with a hydrocarbon layer. The processes and chemical reactions will be analyzed later on in this section.

The product-ion translational energy with samples at room temperature changed, in comparison with the heated samples,

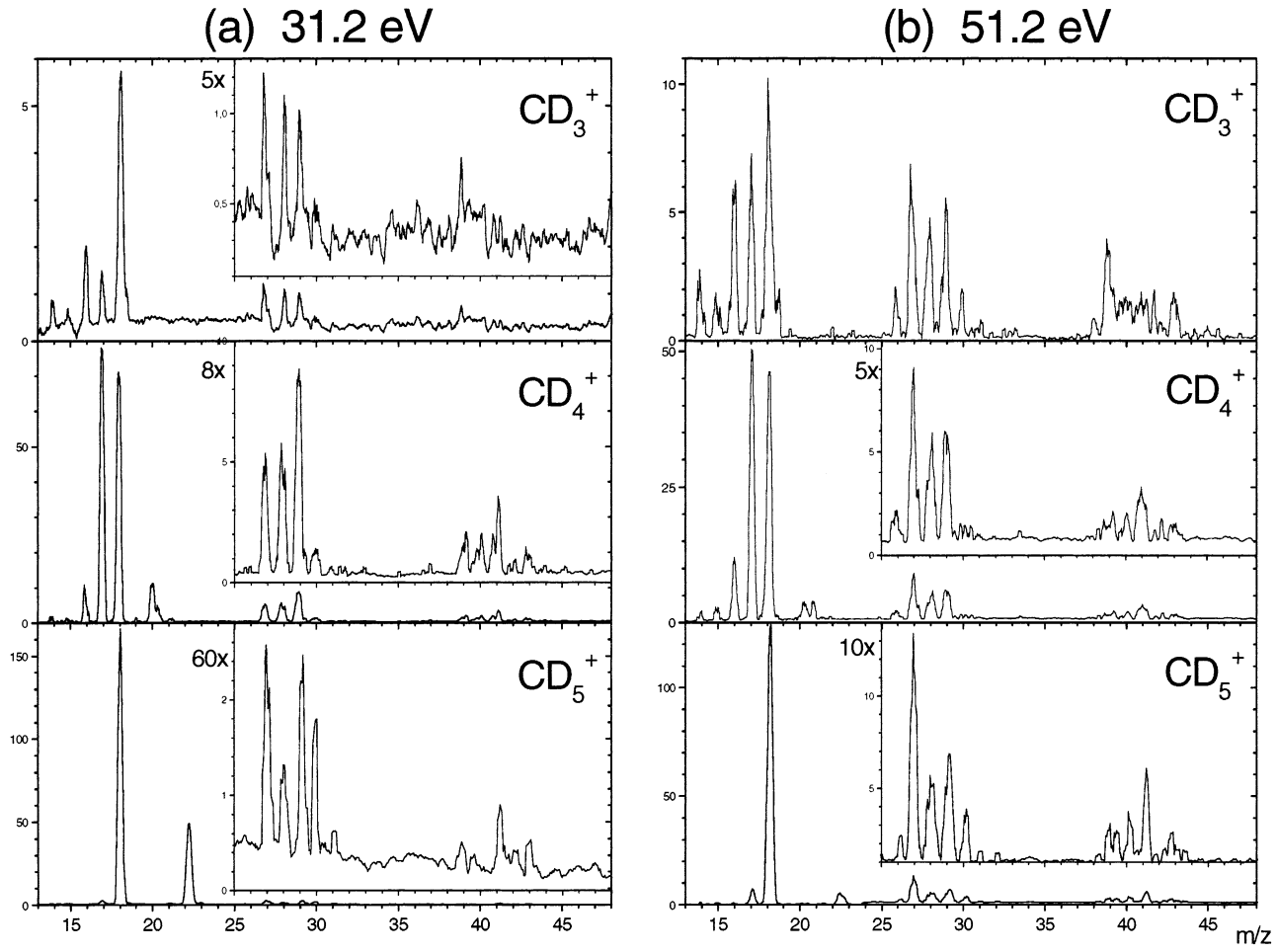

Figure 6. Mass spectra of product ions from collisions of projectile ions CD_3^+, $CD_4^{+\bullet}$, and CD_5^+ with a HOPG surface at room temperature. Collision energies were (a) 31.6 eV and (b) 51.6 eV; incident angle $\Phi_N = 60°$. Insets show upper portions of the mass spectra with increased sensitivity.

too. For example, for the incident ion CD_5^+ (Figure 7) and incident energy of 51.6 eV, the peak of the translational energy distribution of the inelastically scattered product CD_5^+ was at 56% of the incident energy (to be compared with 75% on the heated HOPG surface). With decreasing incident energy, this ratio decreased to 49% and 41% at 31.6 and 16.6 eV, respectively. Thus collisions with the HOPG at room temperature exhibit larger inelasticity than with the heated surface. The angular distributions of the product ions (Figure 8) were somewhat broader and the maximum shifted to slightly larger angles 75°−78° (closer to the surface).

An analogous, more dramatic effect of a clean vs contaminated surface on inelasticity of surface collisions was observed earlier[16] for collisions of the large polyatomic ion C_{60}^+ (incident energy 200 eV, incident angle 45°) with a clean and hydrocarbon-covered HOPG surface. While the product ions C_{60}^+ scattered from the clean HOPG surface retained 23% of the incident energy, C_{60}^+ scattered inelastically from a hydrocarbon-covered HOPG surface had only 5% of the incident energy.

3.5. Chemical Reactions in Collisions with HOPG at Room Temperature. The most probable reaction with the surface material appears to be the reaction of H-atom transfer between the projectile radical cation $CD_4^{+\bullet}$ and surface hydrogen leading to CD_4H^+ and its dissociation products CD_2H^+ and CD_3^+

$$CD_4^{+\bullet} + H{-}S \rightarrow CD_4H^+ (+ S^\bullet) \rightarrow CD_2H^+ + D_2;\quad CD_3^+ + HD \quad (3)$$

From the ion intensities in the spectra (Table 1 and Figure 6), one can roughly estimate that reaction 3 was, in the incident energy range investigated, about 3 times more effective than $CD_4^{+\bullet}$ surface dissociation and about 10 or more times more effective than a reaction in which C_2 product ions were formed.

The ion product CD_2H^+ could be observed also in collisions of CD_3^+ and CD_5^+ at high incident energies (51.6 eV). It was presumably formed in isotope-exchange interactions of the projectile with surface hydrogen.

In the analysis of the C_2 product ions, the spectra obtained with the CH_n^+ ($n = 3, 4, 5$) projectiles were compared with the spectra of the $^{13}CH_n^+$ projectiles to assess the ratio of product ions $C_2H_n^+$ formed by simple sputtering of the surface material and product ions $^{13}CCH_n^+$ resulting from the interaction of the ^{13}C labeled projectiles with the surface carbon and hydrogen. This analysis (Table 3) showed for the collision energy of 31.6 eV that about 25% ± 5% (percent of the total C_2 ion yield) of $C_2H_3^+$ were sputtered ions and 40−50% were reaction products containing ^{13}C. On the other hand, about 15−20% (of the total C2 yield) of $C_2H_5^+$ resulted from surface sputtering and a smaller fraction of 5−7% (about 3 times smaller than the sputtered fraction) appeared to be reaction products, possibly precursors of $C_2H_3^+$. Formation of ions $C_2H_2^+$ and $C_2H_4^+$ (4−5% of the total C_2 ion yield) was regarded as nonsignificant, resulting presumably from further dissociation of the primary products. The main C_2 product of chemical reactions between the projectile ion and the surface material was thus clearly the

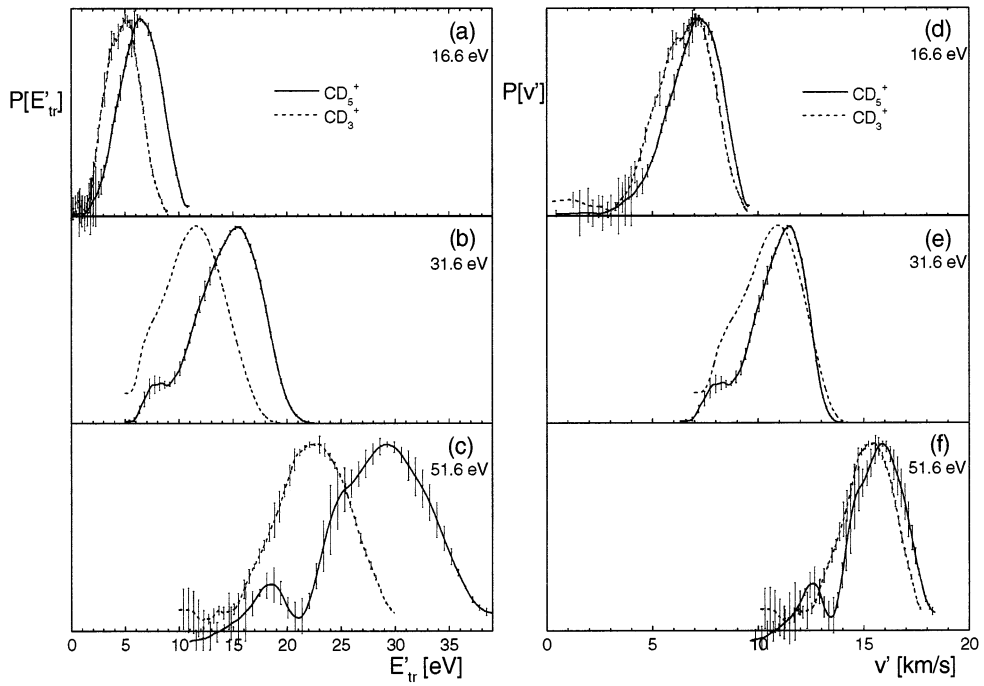

Figure 7. Distribution of (a−c) translational energy, $P(E'_{tr})$, and (d−f) velocity, $P(v')$, of product ions CD_5^+ (full line) and CD_3^+ (dashed line) from collisions of CD_5^+ with a HOPG surface at room temperature. Collision energies were (a, d) 16.6 eV, (b, e) 31.6 eV, and (c, f) 51.6 eV; incident angle $\Phi_N = 60°$, measured at the product scattering angle $\Phi'_N = 74°$.

TABLE 3: Fraction of Sputtering vs Reaction at Surface for C_2-Group at Incident Energy of 31.6 eV and 16.6 eV

	projectile					
	CH_3^+, $^{13}CH_3^+$		$CH_4^{+\bullet}$, $^{13}CH_4^{+\bullet}$		CH_5^+, $^{13}CH_5^+$	
product	sputtering	reaction	sputtering	reaction	sputtering	reaction
			31.6 eV			
C_2H_2, $^{13}CCH_2$		12.8		7.1		4.3
C_2H_3, $^{13}CCH_3$	24.8 ± 4	39.4 ± 4	24.0 ± 5	50.4 ± 5.8	25.3 ± 3	40.8 ± 3
C_2H_4, $^{13}CCH_4$		6.4		4.5		3.6
C_2H_5, $^{13}CCH_5$	14.8 ± 5	4.8	13.1 ± 6	6.8	21.8 ± 3	7.5
			16.6 eV			
C_2H_2, $^{13}CCH_2$						
C_2H_3, $^{13}CCH_3$			11.9 ± 4.9	67.1 ± 8.3	31.3 ± 0.3	13.1 ± 0.3
C_2H_4, $^{13}CCH_4$						10.8
C_2H_5, $^{13}CCH_5$			16 ± 8	11.8	33.5 ± 0.4	7.3

$C_2H_3^+$ ion. Analogous analysis at the collision energy of 16.6 eV did not contradict these conclusions (Table 3). Formation of this ion product in collisions of various organic projectiles with surfaces has been observed earlier, too.[2,3,22]

The ion intensities of the C_2 group of ion products resulting from collisions of CD_3^+, $CD_4^{+\bullet}$, and CD_5^+ (collision energies 16.6 and 31.6 eV) with the surface were then corrected for the contributions of the sputtered ions to yield net intensities of ions $C_2H_2D^+$ and $C_2HD_2^+$ resulting from chemical reactions with the surface. The relative ratios of these two product ions, each resulting from an analysis of a series of spectra, are given in Table 4. The data show that the ratio $C_2H_2D^+/C_2HD_2^+$ for collisions of CD_3^+ approached the value of 2:1 (2.33), for collisions of $CD_4^{+\bullet}$ the value of 1:1 (0.94), and for collisions of CD_5^+ the value of 2:3 (0.70). In the case of $C_2HD_2^+$ for CD_3^+, 16.6 eV (in parentheses), data for the sputtering contribution was missing, and it was taken as a mean value of sputtering vs chemical reaction for projectiles $CD_4^{+\bullet}$ and CD_5^+ (see spectra in Table 1).

The ratios $C_2H_2D^+/C_2HD_2^+$ make it possible to estimate the number of D and H atoms involved in the $C_2X_3^+$ (X = H, D) product-ion formation and to suggest a mechanism for formation of this product ion in collisions of the three projectile ions with the HOPG surface at room temperature. It appears that a common feature is involvement of the terminal CH_3 group of the surface hydrocarbons in the $C_2X_3^+$ product formation and attachment of one $D^\bullet$ atom of the projectile to the $C^\bullet H_2$ hydrocarbon residue on the HOPG surface. The mechanisms of the processes that lead to the formation of the $C_2X_3^+$ product in collisions with HOPG surface at room temperature can be then formulated as (-**S** stands for surface, the ratios in parentheses show the expected $C_2H_2D^+/C_2HD_2^+$ ratios consistent with this mechanism)

$$CD_3^+ + CH_3{-}CH_2\text{-}\mathbf{S} \rightarrow CH_2D\text{-}\mathbf{S} + [CD_2CH_3]^+ \rightarrow (C_2H_2D^+ + X_2)/(C_2HD_2^+ + X_2);\quad (2{:}1)\quad (4)$$

$$CD_4^{+\bullet} + CH_3{-}CH_2\text{-}\mathbf{S} \rightarrow CH_2D\text{-}\mathbf{S} + [CD_3CH_3]^{+\bullet} \rightarrow (C_2H_2D^+ + X_2 + X^\bullet)/(C_2HD_2^+ + X_2 + X^\bullet);\quad (1{:}1)\quad (5)$$

$$CD_5^+ + CH_3{-}CH_2\text{-}\mathbf{S} \rightarrow CH_2D\text{-}\mathbf{S} + [CD_4CH_3]^+ \rightarrow (C_2H_2D^+ + 2X_2)/(C_2HD_2^+ + 2X_2);\quad (2{:}3)\quad (6)$$

Energetics of the processes involved was calculated from gas-phase thermochemical data.[23] It turns out that the reaction heats of the projectile ions with the terminal CH_3- group of gas-phase alkanes C_2 to C_9 are about the same because of a

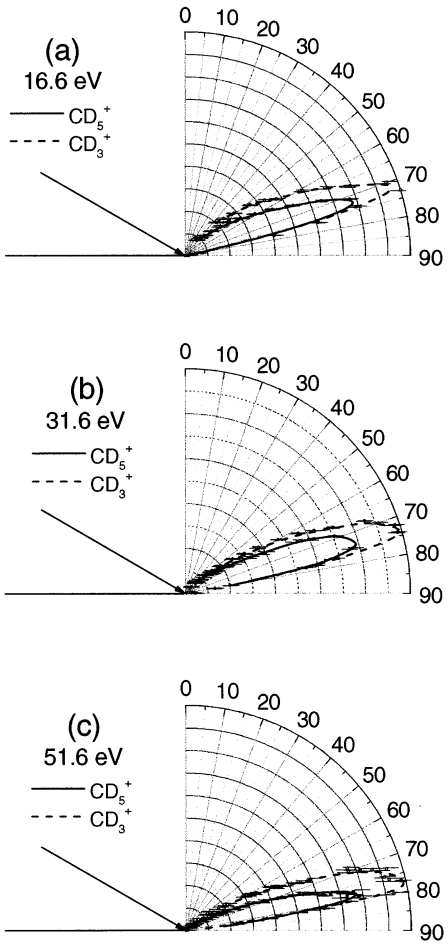

Figure 8. Angular distributions of product ions CD_5^+ (full line) and CD_3^+ (dashed line) from collisions of CD_5^+ with a HOPG surface at room temperature. Incident energies were (a) 16.6 eV, (b) 31.6 eV, and (c) 51.6 eV; incident angle $\Phi_N = 60°$.

TABLE 4: Ratios of the Neat Chemical Reaction Contribution to Intensities of the Product Ions $C_2H_2D^+$ and $C_2D_2H^+$

31.6 eV			
projectile	$C_2H_2D^+$	$C_2D_2H^+$	$C_2H_2D^+/C_2D_2H^+$
CD_3^+	31.5 ± 3.2	13.5 ± 2.5	2.33
$CD_4^{+\bullet}$	25.3 ± 1.8	26.8	0.94
CD_5^+	14.6 ± 2.2	20.65 ± 3.1	0.7
16.6 eV			
projectile	$C_2H_2D^+$	$C_2D_2H^+$	$C_2H_2D^+/C_2D_2H^+$
CD_3^+	20.1 ± 2.5	$(9.7 \pm 3.5)^a$	2.1
$CD_4^{+\bullet}$	28.9	34 ± 5	0.85

[a] Data for the sputtering contribution was missing, and it was taken as a mean value of sputtering vs chemical reaction for projectiles $CD_4^{+\bullet}$ and CD_5^+.

practically constant difference between the heats of formation of the neighboring alkanes or alkanes C_nH_{2n+2} and the respective radicals $C_nH_{2n+1}^{\bullet}$. Thus, reaction 3 with terminal hydrogen of C_2-C_9 alkanes is exoergic by about 34 kJ/mol, and this value could be used as at least a rough estimation of the reaction heat of CD_4^+ with surface-adsorbed hydrocarbons. Similarly, one can estimate that in reactions 4−6 the formation of the intermediates $[CD_2CH_3^+]$, $[CD_3CH_3^+]$, and $[CD_4CH_3^+]$ will be exoergic, but the formation of the final products $C_2X_3^+$+, will be endoergic by about 35 kJ/mol (reaction 4), 210 kJ/mol (reaction 5), and 227 kJ/mol (reaction 6). However, the surface collision may be expected to provide sufficient incident-to-internal energy transfer to overcome this barrier,[8] as also suggested by the extensive dissociation of the CD_4H^+ product (reaction 3) to CD_3^+ and CD_2H^+.

The C_3 group could be analyzed only approximately because of the low product-ion intensities. It appears that the $C_3X_3^+$ ions are mostly products of chemical reactions of the projectile with the surface material, while $C_3X_5^+$ are largely products of sputtering of the surface material.

4. Conclusions

(1) Interaction of small hydrocarbon ions CD_3^+, $CD_4^{+\bullet}$, and CD_5^+ and their H and ^{13}C isotopic variants with room-temperature and heated HOPG surfaces was investigated over the collision energy range of 16−52 eV and at the incident angle 60° (with respect to the surface normal). Mass spectra, translational energy distributions, and angular distributions of product ions were measured.

(2) Collisions with the HOPG surface at room temperature showed both processes of surface-induced dissociation and chemical reactions with surface material. All projectiles showed, besides a fraction of sputtered ions, formation of $C_2X_3^+$ (X = H, D) in chemical reactions of the projectile with the surface terminal CH_3- groups; in addition collisions of $CD_4^{+\bullet}$ led to the CD_4H^+ product ion by H-atom transfer with hydrogen of the surface hydrocarbons. Besides that, C_3 products were formed in small quantities.

(3) The inelasticity of surface collisions of these projectile ions with the room-temperature surface was lower than that with larger polyatomic ions (for ethanol cation peak value of $E'_{tr} \approx$ 30% E_{tr}, for example, for CD_5^+ $E'_{tr} \approx 41-55\%$ E_{tr}), and the peak of angular distribution was at a subspecular angle of 72°−75°.

(4) Heating of the HOPG surface to 600° C reduced the amount of surface hydrocarbons more than 100 times, as indicated by the disappearance of the chemical reactions with the surface material, that is, it practically removed the surface hydrocarbon layer.

(5) Collisions with the heated surface showed only simple dissociation of the projectile ions, and the inelasticity of the surface collisions was smaller (i.e., for CD_5^+ peak value of $E'_{tr} \approx 75\%$ E_{tr}).

(6) The estimated ion survival probability was highest for the CD_5^+ projectile (∼12%), while for CD_3^+ and the radical cation $CD_4^{+\bullet}$, it was about 30−60 times smaller (0.2−0.4%). The percentage of the surviving ions on the heated surfaces was similar.

Acknowledgment. Partial support of this work by the Grant Agency of the Czech Republic (Grant No. 203/00/0632) is gratefully acknowledged. The research has been carried out within the framework of the Association EURATOM-IPP.CR. This paper is dedicated to John C. Tully on the occasion of his sixtieth birthday.

References and Notes

(1) Rabalais, J. W., Ed. *Low Energy Ion-Surface Interactions*; John Wiley: New York, 1994.

(2) Cooks, R. G.; Ast, T.; Mabud, M. D. A. *Int. J. Mass Spectrom. Ion Processes* **1990**, *100*, 209.

(3) Grill, V.; Shen, J.; Evans, C.; Cooks, R. G. *Rev. Sci. Instrum.* **2001**, *72*, 3149.

(4) Hofer, W. O., Roth, J., Eds. *Physical Processes of the Interaction of Fusion Plasma with Solids*; Academic: San Diego, CA, 1996.

(5) Žabka, J.; Dolejšek, Z.; Herman, Z. *J. Phys. Chem B*, in press.

(6) Kubišta, J.; Dolejšek, Z.; Herman, Z. *Eur. Mass Spectrom*. **1998**, *4*, 311.

(7) Wörgötter, R.; Kubišta, J.; Žabka, J.; Dolejšek, Z.; Märk, T. D.; Herman, Z. *Int. J. Mass Spectrom. Ion Processes* **1998**, *174*, 53.

(8) Žabka, J.; Dolejšek, Z.; Roithová, J.; Grill, V.; Märk, T. D.; Herman, Z. *Int. J. Mass Spectrom*. **2001**, *213*, 145.

(9) Sugai, H.; Mitsuoka, Y.; Toyoda, H. *J. Vac. Sci. Technol., A* **1998**, *16*, 290.

(10) Quayyum, A.; Mair, C.; Schustereder, W.; Goehlich, A.; Goehlich, A. L.; Scheier, P.; Herman, Z.; Märk, T. D. In *OPG 2001*; Proceedings of the 51st Meeting of the Austrian Physical Society, Vienna, Austria; OPG: Vienna, Austria, 2001; p 100.

(11) Morris, J. R.; Kim, G.; Barstis, T. L. O.; Mitra, R.; Jacobs, D. C. *J. Chem. Phys.* **1997**, *107*, 6448.

(12) Maazous, M.; Barstis, T. L. O.; Maazous, P. L.; Jacobs, D. C. *Phys. Rev. Lett.* **2000**, *84*, 1331.

(13) Koppers, W. R.; Beijersbergen, J. H. M.; Weeding, T. L.; Kistemaker, P. G.; Kleyn, A. W. *J. Chem. Phys.* **1997**, *107*, 10736.

(14) Koppers, W. R.; Gleeson, M. A.; Lourenco, J.; Weeding, T. L.; Los, J.; Kleyn, A. W. *J. Chem. Phys.* **1999**, *110*, 2588.

(15) Los, J.; Gleeson, M. A.; Koppers, W. R.; Weeding, T. L.; Kleyn, A. W. *J. Chem. Phys.* **1999**, *111*, 11080.

(16) Beck, R. D.; Rockenberger, J.; Weiss, P.; Kappes, M. M. *J. Chem. Phys.* **1996**, *104*, 3638.

(17) Wainhaus, S. B.; Lim, H.; Schultz, D. G.; Hanley, L. *J. Chem. Phys.* **1997**, *106*, 10329.

(18) von Koch, H.; Lindholm, E. *Ark. Fys*. **1961**, *21*, 123.

(19) Čermák, V.; Herman, Z. *Nucleonics* **1961**, *19*, 106.

(20) Stockbauer, R. *J. Chem. Phys*. **1973**, *58*, 3800.

(21) Vestal, M. In *Fundamental Processes in Radiation Chemistry*; Ausloos, P., Ed.; Wiley: New York, 1968; p 110.

(22) Winger, B. J.; Lane, H. J.; Hornig, R. S.; Julian, R. K., Jr.; Lammert, S. A.; Riederer, D. E., Jr.; Cooks, R. G. *Rev. Sci. Instrum*. **1992**, *63*, 5613.

(23) Lias, S.; Bartmess, J. E.; Liebman, J. F.; Holmes, J. L.; Levin, R. D.; Mallard, W. C. *J. Phys. Chem. Ref. Data* **1988**, *17*, Suppl. 1.